Neuron, Vol. 15, 1193–1201, November, 1995, Copyright © 1995 by Cell Press

CAG Expansion Affects the Expression of Mutant Huntingtin in the Huntington's Disease Brain

Neil Aronin,* Kathryn Chase,* Christine Young,* Ellen Sapp,† Cordula Schwarz,† Nahida Matta,‡ Ruth Kornreich,‡ Bernhard Landwehrmeyer,† Edward Bird,† M. Flint Beal,† Jean-Paul Vonsattel,§ Tom Smith,‖ Robert Carraway,# Frederick M. Boyce,† Anne B. Young,† John B. Penney,† and Marian DiFiglia†

*Department of Medicine and Department of Cell Biology
‖Department of Pathology
#Department of Physiology
University of Massachusetts Medical Center
Worcester, Massachusetts 01655
‡Dianon Systems, Inc.
200 Watson Boulevard
Stanford, Connecticut 06497
†Department of Neurology
§Department of Pathology
Massachusetts General Hospital
Harvard Medical School
Boston, Massachusetts 02114

Summary

A trinucleotide repeat (CAG) expansion in the huntingtin gene causes Huntington's disease (HD). In brain tissue from HD heterozygotes with adult onset and more clinically severe juvenile onset, where the largest expansions occur, a mutant protein of equivalent intensity to wild-type huntingtin was detected in cortical synaptosomes, indicating that a mutant species is synthesized and transported with the normal protein to nerve endings. The increased size of mutant huntingtin relative to the wild type was highly correlated with CAG repeat expansion, thereby linking an altered electrophoretic mobility of the mutant protein to its abnormal function. Mutant huntingtin appeared in gray and white matter with no difference in expression in affected regions. The mutant protein was broader than the wild type and in 6 of 11 juvenile cases resolved as a complex of bands, consistent with evidence at the DNA level for somatic mosaicism. Thus, HD pathogenesis results from a gain of function by an aberrant protein that is widely expressed in brain and is harmful only to some neurons.

Introduction

Huntington's disease (HD) is an autosomal dominant disorder that causes progressive impairment of cognitive and motor functions, significant forebrain atrophy, and severe loss of neurons, particularly in the striatum. The disease leads to incapacitation and premature death (Dunlap, 1927; Vonsattel et al., 1985; Folstein, 1989; Young, 1994). Patients with adult onset HD manifest clinical signs by the age of 40, run a clinical course of 15–20 years, and exhibit choreiform movements; rigidity is more characteristic of the rarer HD phenotype of children, which has a shorter course of 7–10 years.

HD belongs to a growing number of inherited disorders in which the mutation is a trinucleotide repeat expansion (Bates and Lehrach, 1994; Willems, 1994). In HD, a CAG repeat at the 5′ end of the coding region of IT15 expands from the normal 6–34 repeats to 38 or more repeats (The Huntington's Disease Collaborative Research Group, 1993). In adult onset HD, the CAG repeat number is generally in the range of 40–50; in juvenile onset HD, however, the repeat number is larger, sometimes exceeding 100. As with other CAG repeat disorders, triplet repeat expansion in HD has been inversely correlated with age of onset and rate of progression (Andrew et al., 1993; Duyao et al., 1993; Snell et al., 1993; Stine et al., 1993). Studies have reported an invariable CAG repeat lengths in the brain and other organ tissues and between different brain regions within the same individual (MacDonald et al., 1993; Zuhlke et al., 1993). One group, however, has identified somatic heterogeneity in the CAG repeat length in the HD brain, with the greatest variation occurring in affected brain regions (cortex and striatum) of juvenile cases (Telenius et al., 1994). A widespread heterogeneity of the CAG repeat in brain has been described recently for other triplet repeat disorders (Chong et al., 1995; Ueno et al., 1995), but no correlation to selective brain pathology has been found.

Immunocytochemical and biochemical evidence shows a widespread distribution of huntingtin, the protein encoded by IT15, and a localization in neuronal cell bodies, fibers, and nerve endings in the normal human brain (DiFiglia et al., 1995; Sharp et al., 1995; Trottier et al., 1995). The consequences of the CAG expansion on huntingtin expression in the HD brain, however, are not clear. Despite the demonstration of both a normal and an expanded protein in HD lymphoblasts (Trottier et al., 1995), a mutant protein predicted by the CAG expansion has not been clearly detected in the brain, raising questions about its existence or stability. HD heterozygotes express the mRNA for the normal and HD alleles in brain (Stine et al., 1995). This indicates that the potential for protein expression exists. Clearly central to understanding the pathogenesis of HD are whether the expanded HD allele leads to an altered protein product in the brain, and whether such a protein distributes preferentially in affected brain regions. Moreover, since a greater expansion of the CAG repeat is associated with a more severe form (early onset) of the illness, it is important to compare the pattern of huntingtin protein expression in children versus adults with HD. Finally, the influence of somatic heterogeneity in CAG repeat length on huntingtin protein expression needs to be explored for its potential role in selective brain pathology.

The goal of this study, therefore, was to determine whether a mutant protein product is expressed in the HD brain and whether its regional distribution or biochemical features can be correlated with genetic, clinical, and neu-

ropathological features of the disease. Our findings show that, in HD heterozygotes, CAG expansion leads to the widespread expression of an altered protein product of increased size throughout the brain. The difference in mobility of mutant huntingtin relative to the wild-type protein correlates with CAG repeat expansion. Furthermore, the mutant protein migrates more broadly than the wild-type protein and in most juvenile cases consists of a complex of bands suggestive of somatic heterogenity in the CAG repeat expansion. The findings support a gain of function as the genetic basis for the disease and strengthen the idea that the pathogenesis of HD is due to the selective vulnerabilty of some neurons to the presence of the mutant protein and its aberrant actions.

Results

Detection of Mutant Huntingtin in HD-Affected Cases: Relationship to CAG Repeat Length

To determine whether an altered form of huntingtin was expressed in the HD brain and how expression was affected by the extent of CAG expansion, we examined huntingtin in synaptosomal preparations of frontal cortex from 22 HD brains (11 adult onset and 11 juvenile onset) and 8 control brains (unaffected; Table 1). Proteins were separated by SDS–polyacrylamide gel electrophoresis (SDS–PAGE) and transferred to nitrocellulose membranes, which were probed with antisera directed against the N-terminus (amino acids 1–17; Ab 1) of huntingtin and an internal protein sequence (amino acids 585–745; Ab 585) downstream from the polyglutamine region. As previously reported (DiFiglia et al., 1995), immunoreactive huntingtin is detected with these antisera at approximately its predicted MW (estimated size is 348 kDa) in synaptosomes from human control cortex. The native protein is also present in heterozygous HD brain of adult and juvenile onset cases (Figure 1). A mutant protein of comparable intensity to the wild type was also seen in the HD brains. The mutant species was distinguishable as a separate protein band in all HD cases except patient A11, who had the smallest expanded allele tested (40 CAG repeats) and a difference from the normal allele of only 15 CAGs. In this case, the mutant protein appeared as a fuzzy upward extension of the wild-type band. The mutant protein was also seen in an HD patient who was presymptomatic at the time of death (Figure 1, case A4) and showed evidence of grade 1 pathology (minimal neuronal loss in the striatum) on postmortem examination. Adult onset cases with identical estimates of CAG repeat expansion showed different degrees of separation of the normal and mutant proteins on the immunoblot. The space between the two bands was invariable when immunoblots were repeated, suggesting that the relationship in electrophoretic mobility between the normal and mutant species was an inherent property of the proteins.

The slower migratory mutant band occurred at various positions above the wild-type protein up to an apparent MW range of 450 kDa for upper alleles with the largest number of CAG repeats. Thus, the increase in apparent size of mutant huntingtin exceeded the actual increase in MW of 2–10 kDa predicted by the expanded polyglutamine region. Computer-assisted image analysis showed that for all HD cases the distance of the peak separation between mutant and wild-type huntingtin protein was highly correlated ($r = 0.84$, $p < .0001$; Pearson correlation coefficient) with the difference in the number of CAG repeats between the normal and mutant alleles (Figure 2). The adult onset HD group alone also exhibited a significant positive correlation ($r = 0.63$, $p < .03$). The results were similar for the two anti-huntingtin antisera (Ab 1 and Ab 585) used in the analysis.

Table 1. Cases Used to Examine Huntingtin in Brain

Case	Sex	Age	Diagnosis/ Grade	Number of CAG Repeats
C1	M	55	Control	17/17
C2	F	93	Control	17/22
C3	M	66	Control	NA
C4	M	78	Control	22/24
C5	M	77	Control	17/17
C6	M	81	Control	15/17
C7	F	35	Control	17/18
C8	M	68	Control	9/17
C9	M	63	Control	NA
A1	M	35	HD4	22/44
A2	F	62	HD3	16/43
A3	M	57	HD2	17/43
A4	F	32	HD1	17/42
A5	M	63	HD3	19/44
A6	F	84	HD3	15/40
A7	M	44	HD3	19/44
A8	F	61	HD3	17/41
A9	M	58	HD3	17/44
A10	M	63	HD3	23/43
A11	F	40	HD2	25/40
A12	F	66	HD3	27/42
J1	F	6	HD3	10/150[a]
J2	F	16	HD	20/67
J3	F	39	HD4	19/65
J4	F	17	HD	17/72
J5	F	28	HD3	15/69
J6	F	12	HD4	17/105
J7	M	17	HD	17/91
J8	M	9	HD	27/90
J9	M	6	HD	18/125[a]
J10	M	19	HD	20/68
J11	F	16	HD3	17/83

Control (C1–C9), adult (A1–A11), and juvenile (J1–J11) HD cases examined in this study. Age indicated is at the time of death. The pathological grade is provided where it was available and is based on the grading system of Vonsattel et al. (1985). A grade of 1 means that there is minimal cell loss in the striatum, and a grade of 4 indicates severe atrophy, neuronal loss in the striatum, and involvement of other brain regions. CAG repeats for the normal and expanded alleles are given for the cortex with a few exceptions in the juvenile cases, where only cerebellar tissue was available. NA, not available.

[a] Based on estimate from Southern blot.

Widespread Expression of Mutant Huntingtin in the Brain

One possible explanation for the region-specific degeneration in HD is that the mutant protein is expressed only in affected brain regions such as the striatum and cortex.

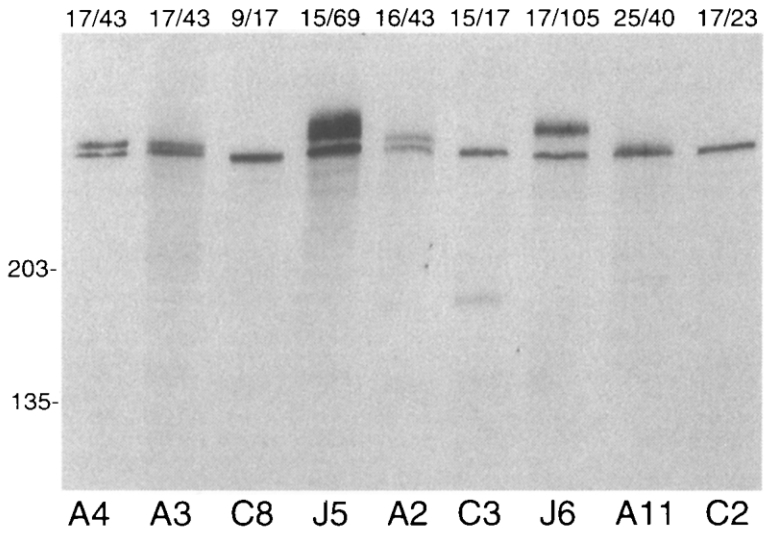

Figure 1. Immunoblots of Control and HD Brain Cortex Synaptosomes Probed with Ab 1

Controls (C2, C3, and C8) and HD cases (A2, A3, A4, A11, J5, and J6) are shown with the CAG repeat length for each pair of alleles indicated at the top. HD case A4 is from a patient who was presymptomatic at the time of death. All cases except for A4 are from the same immunoblot. The mutant protein runs as a separate band in all HD cases except A11, which had the smallest expanded allele examined. Protein concentrations varied from 10 to 25 μg per lane. Molecular weight standards in kilodaltons are shown on the left.

Therefore, we compared huntingtin expression in a variety of cortical and subcortical gray and white matter regions in a control case, an adult HD case, and a juvenile HD case (case J11). Detection of native huntingtin in the control case (Figure 3A) showed a similar signal throughout all gray matter areas examined. Similarly, in the HD-affected brain (Figure 3B), mutant huntingtin was detected along with the wild-type protein in all areas of gray matter in both the juvenile (Figure 3B) and adult onset (data not shown) patients. In addition to its widespread expression in gray matter, a relatively strong signal for huntingtin was detected in some regions of white matter, particularly the subcortical white matter, the centrum semi-ovale, and the corpus callosum in both the normal and HD brain. In general, forebrain regions produced stronger expression of mutant huntingtin than hindbrain areas in the HD brain.

The HD cerebellum consistently exhibited a weaker signal in both wild-type and mutant protein expression than the cortex in a series of adult and juvenile HD cases where the two regions were compared (Figures 4A and 5). Manipulation of protein concentration and the method of protein extraction (total extracts versus synaptosomes) did not account for the weaker signal in the cerebellum. Analysis of hematoxylin- and eosin-stained sections of the cortex and cerebellum available for 3 of the cases (J5, J7, and J10) showed that the density of neurons in the cerebellum was comparable to that of controls and was mildly to moderately reduced in regions of the cortex of these cases (data not shown).

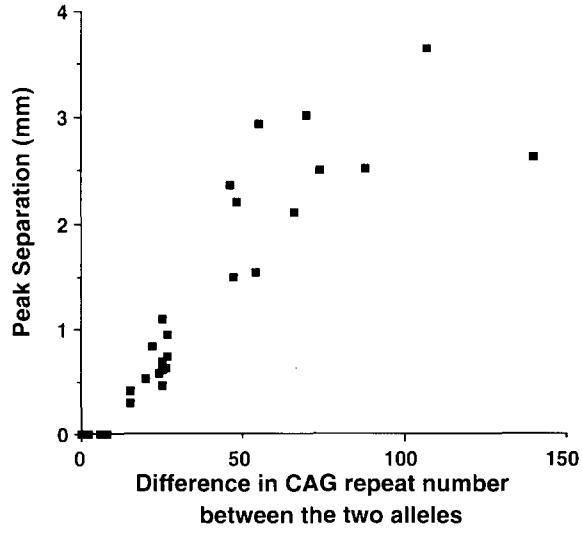

Figure 2. Comparison of CAG Repeat Length and the Difference in Migration of Immunoreactive Huntingtin Protein Peaks in Cortex Synaptosomes

CAG repeat length is plotted as the difference in size between the two alleles. The migration of wild-type and mutant huntingtin is indicated as the distance in millimeters between protein bands as determined by computer-assisted image analysis. The difference in peak separation in the control cases is assumed to be zero since only one peak could be detected. For all cases, $r = 0.89$ with $p < .0001$; if control cases are not included, $r = 0.84$ with $p < .0001$. For adult HD only, $r = 0.64$, $p < .03$; for juvenile HD only, $r = 0.59$, not significant.

Mutant Huntingtin Migrates as a Broad Band: Evidence for Somatic Mosaicism

The mutant protein migrated more broadly than the wild type. To compare the relative expression of the two protein products in each HD case, the normal and mutant proteins were quantified by measuring the absolute breadth (width) and the relative amount (integrated area of the density plot) of each band. Immunoblots showed that the signal of mutant huntingtin was significantly broader in size (width, $p < .001$, t test, paired comparisons) and greater in overall integrated area (integrated area, $p < .001$, t test, paired comparisons) than the corresponding wild-type huntingtin (Table 2). These differences were found with both antisera. The patterns of change in mutant and wild-type huntingtin were more pronounced in juvenile than in adult cases; this finding was especially robust with use of the N-terminal antisera (Ab 1; Table 2).

The broad band characteristic of mutant huntingtin was most striking in cortex and least apparent in the cerebel-

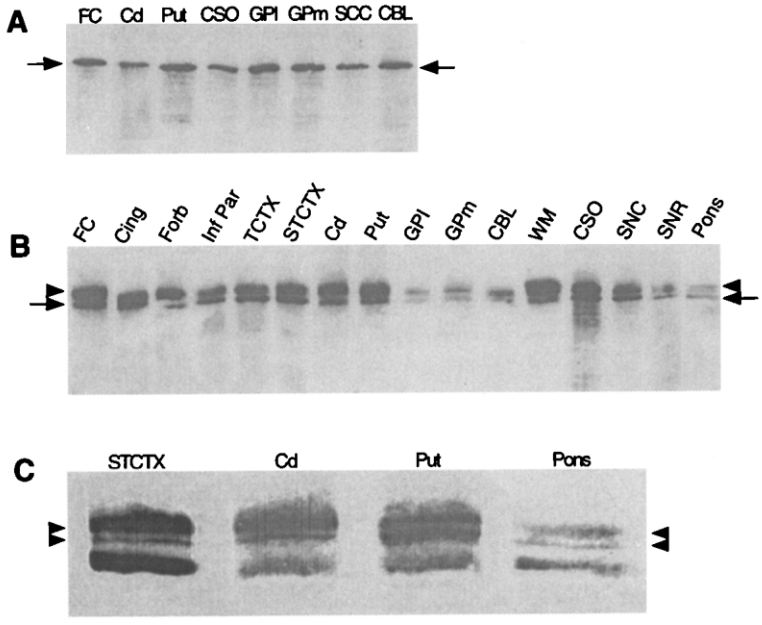

Figure 3. Regional Distribution of Huntingtin in Control and HD Brain

(A) Immunoblot of P2 fractions (20 μg/lane) from 8 regions of control brain (case C9) probed with Ab 1. The native protein (arrow) is detected in all regions of gray and white matter sampled.

(B) Immunoblots of P2 fractions (20 μg/lane) from a juvenile HD (case J11) brain show the presence of both the normal (arrows) and mutant (arrowheads) proteins in all regions, including both gray and white matter. The mutant protein appears as intense as the coexpressed normal protein but is more broadly distributed in the cortex, caudate, putamen, substantia nigra, and white matter regions. The panel is compiled from three immunoblots processed at the same time with similar exposures. Protein extractions, separations, and immunoblotting conditions were the same in the control and HD cases.

(C) Less exposed images of some of the same regions shown in (B). Note the presence of multiple bands in both more affected (caudate and putamen) and less affected (striate cortex and pons) areas.

CBL, cerebellum; Cd, caudate; Cing, cingulate cortex; CSO, centrum semi-ovale; FC, frontal cortex; Forb, frontal orbital; GPl, lateral globus pallidus; GPm, medial globus pallidus; Inf Par, inferior parietal cortex; Put, putamen; SCC, splenium of the corpus callosum; SNC, substantia nigra, pars compacta; SNR, substantia nigra, pars reticulata; STCTX, striate cortex; TCTX, temporal cortex; WM, subcortical white matter.

lum, particularly in the juvenile cases (Figures 4A and 5). A quantitative comparison of the cortex and cerebellum in a group of adult and juvenile cases confirmed that there was a larger ratio of the integrated area of the mutant to wild-type bands (area ratio) in the cortex than in the cerebellum in both the adult ($p < .001$, t test, paired comparisons) and juvenile ($p < .001$) cases (see Figure 4C). Reducing the amount of protein analyzed in the cortical sample from 20 to 2 μg did not alter the broadness of the mutant band (data not shown), indicating that the larger size was not dependent on the amount of protein loaded.

In the cortex of 6 of the 11 juvenile cases examined, we noticed that, at brief film exposures of the chemiluminescent reaction, mutant protein was resolved as two or three distinct bands. This heterogeneity in mutant huntingtin was seen in cases J11 (see Figure 3C), J5 (see Figure 4B), J2 (see Figure 5), J8, and J10. In contrast to the cortex, the cerebellum exhibited multiple mutant bands in only 2 of the 11 juvenile HD patients, cases J1 (see Figure 4B) and J10. Of the 16 regions examined in case J11, two distinct mutant bands were discernible in most brain areas, including all areas of the cortex, the subcortical white matter, the caudate, putamen, substantia nigra, and pons but not the cerebellum (see Figure 3C). Thus, both affected (cortex and striatum) and unaffected (pons and cerebellum) brain regions in HD may exhibit heterogeneity in mutant huntingtin expression; the cerebellum is a region where the occurrence of multiple mutant species is very low.

To determine whether somatic mosaicism in CAG repeat length of the expanded HD allele (Telenius et al., 1994) accounted for the heterogeneity in mutant huntingtin, we selected 2 juvenile and 2 adult onset cases in which the mutant protein appeared broader in the cortex than in the cerebellum. The broad mutant protein in 1 of the juvenile cases (J5) showed three distinct bands, while that in the other case (J6) did not (see Figure 4A). Consistent with previous findings (Telenius et al., 1994), the cortex in both juvenile cases (Figure 6, case J5) exhibited a greater spread in the polymerase chain reaction (PCR) smear (25%–50% increased span) and a displacement upward of the estimated major allele band compared with the cerebellum (69 versus 62 in case J5 [see Figure 5]; 105 versus 95 in case J6). In the 2 adult onset cases, the range of bands was small and similar in both regions, with the major band being identical in the 2 brain regions (42 versus 42 in case A4; 43 versus 43 in case A2; data not shown). Thus, it appears, at least in the juvenile cases, that the increased size and heterogeneity (multiple bands) in mutant huntingtin can be explained by the presence at the DNA level of greater heterogeneity and larger repeat lengths of the HD allele in the cortex than in the cerebellum. The absence of a similar relationship in the adult cases between genomic DNA heterogeneity and mutant huntingtin expression may be due to limitations in the sensitivity of the PCR assay. Somatic mosaicism of CAG repeat length in adult onset HD brain is less obvious than in juvenile cases (Telenius et al., 1994). Also, other tissue-specific factors involved with posttranslational processing may contribute to the broader spread of mutant huntingtin in the brain.

Assessment of Other Factors Possibly Contributing to the Broad Spread of Mutant Protein

To assess whether N-glycosylation or incomplete denaturation of mutant huntingtin contributed to its broader size, synaptosome extracts from the cortex and cerebellum of

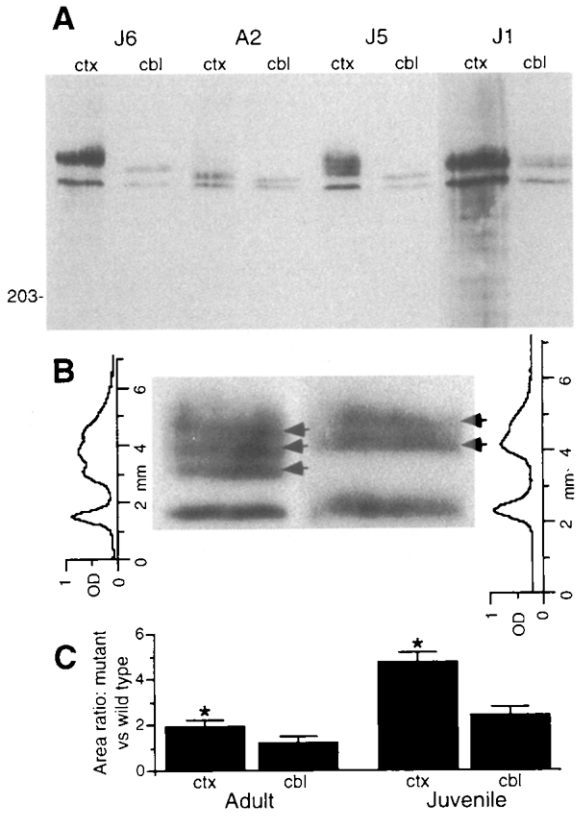

Figure 4. Comparison of Huntingtin in Cortex and Cerebellum of the HD Brain

(A) Immunoblot of 1 adult onset case (case A2) and 3 juvenile onset cases (J1, J5, and J6). J1 is taken from a different gel than the other cases. The CAG repeat length is shown at the top. A total of 20 μg of synaptosomal protein was loaded in each lane.

(B) Higher magnification of cortex from case J5 (left) and of cerebellum from case J1 (right) shows the presence of multiple bands (arrows) in mutant huntingtin. Adjacent optical density plots for each case show the resolution of the wild-type and mutant bands. Multiple mutant bands were much more frequent in the cortex (6 of 11 cases) than in the cerebellum (2 of 11 cases) of the juvenile HD brain.

(C) Comparison of the mean area/intensity ratio of mutant versus wild-type huntingtin in the cortex and cerebellum of 6 adult and 7 juvenile onset cases. Vertical bars indicate SEM. In both the adult and juvenile cases, the area ratio is significantly different between the cortex and the cerebellum. Asterisk denotes $p < .001$ (t test on paired comparisons).

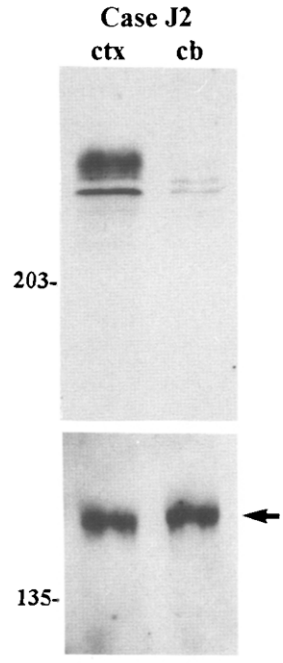

Figure 5. Comparison of Immunoreactive Huntingtin in the Cortex and Cerebellum of Juvenile Case J2

A total of 20 μg of synaptosomal extracts was loaded in each lane. The cortex produces a stronger signal on the immunoblot than the cerebellum for both wild-type and mutant protein. The signal for the 160 neurofilament protein reprobed on the same blot shown below (arrow) is about the same for each region. Molecular weight sizes (kilodaltons) are shown on the left.

the same 2 juvenile onset cases (J5 and J6) were treated with N-glycosidase F or 4 M urea prior to SDS–PAGE and immunoblot. No change in the broad band characteristic of mutant huntingtin was evident with either treatment condition (Figure 7).

Ubiquitin is an 8.5 kDa protein that conjugates to proteins undergoing proteolytic degradation (Carlson et al., 1987). Since ubiquitinated proteins react as a "smear" on immunoblots (Morishima-Kawashima et al., 1993) and ubiquitin-positive dystrophic neurites are found in the HD cortex (Cammarata et al., 1993), we investigated whether the broad mutant huntingtin band seen in the juvenile HD cor-

Table 2. Analysis with Ab 1 of Huntingtin Protein Products in the Control and HD Brain

	n	Peak Separation (mm)	Width (mean ± SEM)		Area (mean ± SEM)	
			Wild Type	Mutant	Wild Type	Mutant
Controls	9	0.0	1.1 ± .05	–	0.21 ± .03	–
Adult onset	12	0.68 ± .06	0.95 ± .05	1.23 ± .07[c]	0.16 ± .03	0.24 ± .05[a]
Juvenile onset	11	2.43 ± .23	1.0 ± .04	2.28 ± .20[d]	0.21 ± .05	0.66 ± .15[b]
All HD	23	1.47 ± .23	0.98 ± .03	1.80 ± .16[d]	0.19 ± .03	0.43 ± .09[c]

[a] Mutant compared with wild type, $p < .05$.
[b] $p < .01$.
[c] $p < .005$.
[d] $p < .0001$.

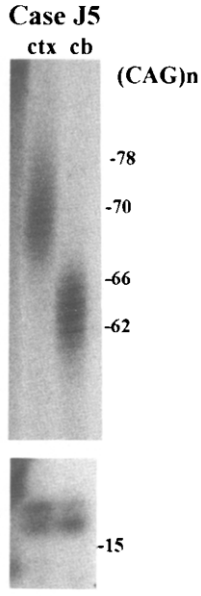

Figure 6. Comparison of CAG Repeat Expansion of the HD Allele in the Cortex and Cerebellum of Case J5 Using a PCR Assay

The cortex yields a product with a greater size of the major band (estimated 69 repeats) and a greater spread of the PCR smear than the cerebellum (major band estimated 62 repeats), providing support for somatic variation. The PCR product from the other allele (shown below) was the same size for both brain regions. Similar results were obtained for case J6. A DNA sequencing ladder was performed with the assay and used to estimate the number of CAG repeats (indicated on the right).

tex was due to ubiquitin conjugation. No evidence for ubiquitin immunoreactivity was identified in the region of mutant huntingtin on immunoblots of synaptosomal extracts from HD cases J5 and J6 when probed directly with a polyclonal anti-ubiquitin antibody. Similarly, when protein extracts of these same cases were incubated with anti-ubiquitin antisera and the immunoprecipitated proteins were immunoblotted with Ab 1, immunoreactive huntingtin was not observed. These results suggest that ubiquitin conjugates do not explain the broad band or complex of bands seen on immunoblots of the juvenile HD cortex.

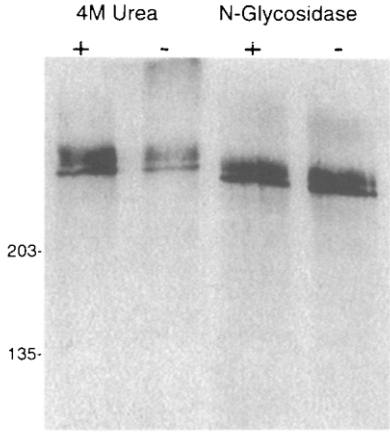

Figure 7. Analysis of the Effect of Denaturation with 4 M Urea and Deglycosylation on the Expression of Mutant Huntingtin in Juvenile Onset Case J5

From left to right: pretreatment with 4 M urea prior to SDS–PAGE (+); no urea control (−); treatment with N-glycosidase-F overnight (+); incubation buffer alone (−). The same results were obtained for case J6. Molecular weight markers are shown on the left.

Discussion

This study has shown that a mutant form of huntingtin is detectable throughout the HD brain and that its increased size in relation to the wild-type protein is highly correlated with CAG repeat expansion. These findings, together with previous evidence for the association of large repeat expansions with early onset and increased clinical severity in HD (Andrew et al., 1993; Duyao et al., 1993; Stine et al., 1993), suggest that the progressive increase in the size of mutant huntingtin is associated with its abnormal function. Mutant huntingtin is not preferentially expressed in regions of known pathology, and thus other factors in conjunction with the presence of the altered protein must contribute to the vulnerability of affected neurons. The detection of mutant huntingtin in synaptosomes indicates that the altered protein is expressed and transported to axon endings at levels similar to those of wild-type protein throughout the brain. The wild-type and mutant huntingtin also exist in the white matter, an observation that has not been previously reported in the normal or HD brain. This localization may include axons and nonneuronal cells and could be important for understanding why there is marked atrophy of the cortical white matter as well as the gray matter in HD brain (De La Monte et al., 1988). Why huntingtin expression in the cerebellum is harder to detect in the HD brain than in the normal brain is unclear. Our ability to see a robust signal for both mutant and wild-type huntingtin in HD brain compared with the detection of only the normal protein by Trottier et al. (1995) may be related to our use of a low bis-acrylamide for SDS–PAGE. During the review of this paper, another group (Ide at al., 1995) reported that the use of lower concentrations of bis-acrylamide significantly improved the detection of an abnormal huntingtin product in HD lympoblasts and cerebral cortex. The expression in brain of a mutant ataxin protein in spinocerebellar ataxia type 1 (Servadio et al., 1995) has also been described. This finding, together with the observations in HD, suggests that the expression in brain of altered proteins from disease genes encoding expanded CAG repeats may be a shared feature of triplet repeat disorders.

Our findings support the view that HD pathogenesis is due to a gain of function in which an aberrant action emerges from the presence of an altered protein in the brain. The mutant protein by our estimates is expressed comparably to the normal protein and is transported to axon endings, where it conceivably has access to the same intracellular targets as the normal huntingtin. In this context, HD may be viewed as a condition where the mutant protein competes with the normal species for intracel-

lular targets. It is likely that the mutant huntingtin possesses at least some normal function. Recent evidence in mice with disrupted IT15 revealed that the embryo dies by day 8.5 (Nasir et al., 1995; Duyao et al., 1995). If the mutant HD were completely dysfunctional, homozygous HD would be incompatible with life. This is not the case; HD homozygotes have a phenotype often indistinguishable from the heterozygous individual (Wexler et al., 1987). Thus, it is likely that the mutant protein shares many of the normal function(s) of the wild-type protein and additionally has encumbered features that lead to aberrant interactions.

Our findings show that the slower mobility (increased size) of mutant huntingtin can be largely attributed to the presence of additional glutamines. Polyglutamine sequences are recognized to be potential sites of protein–protein interactions, and the aberrant expansion of these regions, particularly as occurs in juvenile HD, may be conducive to the formation of deleterious protein complexes (Perutz et al., 1994). The increased size of mutant huntingtin in brain appears to exceed the MW predicted by the addition of extra glutamines, suggesting that the expansion causes a conformational change in the mutant protein. Similar conclusions are suggested from the study of HD lymphoblasts and the in vitro expression of huntingtin with variable CAG repeat lengths in COS cells (Trottier et al., 1995). Altered mobility suggestive of a conformational change has also been described for the mutant gene product in dentatorubral-pallidoluysian atrophy brain (Yazawa et al., 1995). In our study, the difference in sensitivity of the two antisera to mutant huntingtin in the juvenile cases may have resulted from changes in epitope presentation brought about by structural changes in the mutant protein.

The broader spread of the mutant protein relative to the wild-type protein can be largely attributed to somatic heterogeneity in CAG repeat length, as first reported with genomic PCR analysis in HD (Telenius et al., 1994), confirmed in this study, and also recently described for other triplet repeat disorders (Chong et al., 1995; Ueno et al., 1995). The strongest support for somatic heterogeneity at the protein level was shown in the juvenile cases in which, under appropriate conditions, distinct bands could be resolved in the mutant protein. This finding provides clear evidence that somatic heterogeneity results in the translation of multiple mutant protein products. We predict that the characteristic of variable protein expression seen for mutant huntingtin in HD also exists for the expanded proteins encoded by other CAG repeat disease genes. Our findings that somatic mosaicism at the protein level is widespread throughout the brain, is evident in juvenile cases, and is least apparent in the cerebellum parallel previous observations at the genomic DNA level (Telenius et al., 1994). We found no support for a causal relationship between somatic variability and HD pathology, since heterogeneity in mutant protein expression occurred in both affected and nonaffected brain areas. However, the more frequent and striking occurrence of mutant protein heterogeneity in forebrain areas that are more degenerated in HD may be significant in contributing to the severity and phenotypic expression of the disease. The cellular origin of the multiple mutant huntingtin protein products is unknown. Proliferating nonneuronal cells are a likely source, particularly in affected areas where neurons are the most depleted. Further study is needed to determine the cellular origin of the variable mutant proteins and their possible regional contribution to pathological and functional changes in HD-affected individuals.

Experimental Procedures

Tissue Procurement

Brain tissue was obtained from the Brain Tissue Resource Center (Belmont, MA), the University of Massachusetts, Department of Neuropathology, and the Massachusetts General Hospital Neuropharmacology Laboratory Brain Bank. All tissue was quickly frozen and stored at −70°C until further analysis. The time between death and brain dissection was variable but was always between 4 and 48 hr. The dissections of neocortex and cerebellar cortex were performed so as to exclude the underlying white matter as much as possible. Control tissue from donors without HD was handled identically. Most of the adult onset HD cases were evaluated for neuropathological status and assigned a grade according to the criteria of Vonsattel et al. (1985). The majority of adult onset cases were grade 3.

Synaptosome Preparation

The protocol of Koenig (1974) was used. The brain tissue was slowly thawed on ice in homogenization buffer containing 0.32 M sucrose with 0.1 M phenylmethylsulfonyl fluoride (PMSF) and 2 mg/ml pepstatin A. After homogenization and centrifugation, the suspension was layered on a discontinuous sucrose gradient (layers 0.32 M, 0.8 M, 1.0 M, 1.2 M, and 1.4 M). The gradient was centrifuged at 65,000 × g for 2 hr. Synaptosomal fractions at the interfaces of 1.0 to 1.2 M were collected and stored at −70°C. P2 fractions were prepared as described by DiFiglia et al. (1995).

Protein Separation and Western Blot Analysis

Protein fractions (fraction C; 10–20 μg per lane) were submitted to SDS–PAGE using a 10% acrylamide gel containing 0.05% bisacrylamide. The 200 kDa standard was allowed to run to the middle of the gel for all runs. Following transfer to nitrocellulose, blots were probed with Ab 1 (0.5 μg/ml), which recognizes N-terminal amino acids 1–17 of huntingtin, or Ab 585 (1:4000), which was raised to residues at positions 585–745 of huntingtin in a region ~540 residues C-terminal to the polyglutamine domain. Most cases were evaluated with both antisera and probed on different blots at least twice. Immunoreactivity was detected using enhanced chemiluminescence (ECL, Amersham). Film autoradiograms were exposed from 2 s to 4 hr.

CAG Repeat Determination

CAG repeat length was analyzed by PCR and Southern blotting of genomic DNA extracted from brain tissue. PCR assays were performed using a procedure and primers described previously (Goldberg et al., 1993) and resolved on denaturing polyacrylamide (sequencing) gels. In a few cases where amplification by PCR was not obtained, Southern blotting was used to estimate the length of CAG repeats. PstI digests of genomic DNA were resolved by agarose gel electrophoresis and transferred to nitrocellulose filters. The filters were probed with a 366 bp genomic fragment, which was prepared by PCR using primers labeled with ^{32}P by random-primed synthesis.

Deglycosylation Assay

Synaptosome extracts (20 μg) from the cortex and cerebellum of 2 juvenile onset cases were treated in 10% SDS, heated to 100°C for 2 min, and treated with incubation buffer (1 M sodium phosphate [pH 7.4], 30 mM EDTA, 0.5% Nonidet P-40, 0.1% 2-mercapto-ethanol, 0.5 mM PMSF, 1 μg/ml pepstatin A) alone or in the presence of N-glycosidase F (PNGase F, Boehringer Mannheim Biochemica) at 37°C overnight. Invertase was used as the control glycosylated protein.

Ubiquitination Protocol

Synaptosomal extracts (10 μg) from HD brains were treated with anti-ubiquitin antibody (mouse monoclonal, 1 μl, DAKO) in NET gel buffer (50 mM Tris [pH 7.5], 0.1% Nonidet P-40, 0.25% gelatin, 0.15 M NaCl, 0.02% sodium azide, 1 mM EDTA). The mixture (total volume of 100 μl) was incubated overnight at 4°C on a rocker. Protein A Sepharose CL-4B (Sigma) was added, and the mixture was incubated for 1 hr at 4°C and then centrifuged at 10,000 × g for 1 min. After three washes in NET buffer, the Sepharose–protein complex was washed in Tris (pH 6.8) and placed into a new tube. SDS loading buffer and the mixture were boiled for 1.5 min prior to loading on a low bis, 10% SDS–polyacrylamide gel. Proteins were transferred to nitrocellulose, and Western blot analysis was performed using Ab 1.

Image Analysis and Statistical Methods

Immunoblots were quantified using computer-assisted image analysis (M1, Imaging Research Inc., St. Catherines, Ontario). A standard density gradient and size calibration scale were set prior to measurement of the autoradiograms. After the images were scanned, a density distribution plot of the protein bands present in each lane was generated and displayed on the computer monitor. The following measurements were defined from the density plot: the location of maximal density of each protein band (peak location); the width (broadness) of each band; and the integrated area of each distribution (area). "Peak separation" was defined as the distance in millimeters between the peak location of two bands present in the same lane. When more than two bands were resolved in a lane, the two lowest bands were used to calculate peak separation. The ratio of the upper (mutant) band to the lower (wild-type) band was calculated using the width (width ratio) and area (area ratio) measurements obtained as described above. Statistical analysis included ANOVA, t tests for paired comparisons, and Pearson product-moment correlations.

Acknowledgments

Correspondence should be addressed to M. D. This work was supported by grants NS16367 (M. D.), NS15655, AG08671 (A. B. Y. and J. B. P.), and NS31579 (N. A.) and by the Diabetes and Endocrinology Research Center (peptide synthesis core facility), University of Massachusetts Medical Center. The authors thank Mr. Lawrence Cherkas and Mr. Patrick Chang for their help with the figures, and Ms. Lisa Kanaley and Mr. Steve Hankins for their help with the brain tissue acquisition.

The costs of publication of this article were defrayed in part by the payment of page charges. This article must therefore be hereby marked "*advertisement*" in accordance with 18 USC Section 1734 solely to indicate this fact.

Received March 20, 1995; revised July 31, 1995.

References

Andrew, S.E., Goldberg, Y.P., Kremer, B., Telenius, H., Theilmann, J., Adam, S., Starr, E., Squitieri, F., Lin, B., Kalchman, M.A., Graham, R.K., and Hayden, M.R. (1993). The relationship between trinucleotide (CAG) repeat length and clinical features of Huntington's disease. Nature Genet. *4*, 398–403.

Bates, G., and Lehrach, H. (1994). Trinucleotide repeat expansions and human genetic disease. BioEssays *16*, 277–284.

Cammarata, S., Caponnetto, C., and Tabaton, M. (1993). Ubiquitin-reactive neurites in cerebral cortex of subjects with Huntington's chorea: a pathological correlate of dementia? Neurosci. Lett. *156*, 96–98.

Carlson, N., Rogers, S., and Rechsteiner, M. (1987). Microinjection of ubiquitin: changes in protein degradation in HeLa cells subjected to heat-shock. J. Cell Biol. *104*, 547–555.

Chong, S.S., McCall, A.E., Cota, J., Subramony, S.H., Orr, H.T., Hughes, M.R., and Zoghbi, H.Y. (1995). Gametic and somatic tissue-specific heterogeneity of the expanded SCA1 CAG repeat in spinocerebellar ataxia type 1. Nature Genet. *10*, 344–350.

De La Monte, S.M., Vonsattel, J.-P., and Richardson, E.P., Jr. (1988). Morphometric demonstration of atrophic changes in the cerebral cortex, white matter, and neostriatum in Huntington's disease. J. Neuropathol. Exp. Neurol. *47*, 516–525.

DiFiglia, M., Sapp, E., Chase, K., Schwarz, C., Meloni, A., Young, C., Martin, E., Vonsattel, J.-P., Carraway, R., Boyce, F.M., and Aronin, N. (1995). Huntingtin is a cytoplasmic protein associated with vesicles in human and rat brain neurons. Neuron *14*, 1075–1081.

Dunlap, C.B. (1927). Pathologic changes in Huntington's chorea. Arch. Neurol. Psychiat. *18*, 867–943.

Duyao, M., Ambrose, C., Myers, R., Novelletto, A., Persichetti, F., Frontail, M., Folstein, S., Ross, C., Franz, M., Abbott, M., et al. (1993). Trinucleotide repeat length instability and age of onset in Huntington's disease. Nature Genet. *4*, 387–392.

Duyao, M.P., Auerbach, A.B., Ryan, A., Perisichetti, F., Barnes, F.T., McNeill, S.M., Ge, P., Vonsattel, J.-P., Gusella, J.F., Joyner, A.L., and MacDonald, M.E. (1995). Inactivation of the mouse Huntington's disease gene homolog *Hdh*. Science *269*, 407–409.

Folstein, S.E. (1989). Huntington's Disease: A Disorder of Families (Baltimore, Maryland: Johns Hopkins University Press), pp. 1–64.

Goldberg, Y.P., Andrew, S.E., Clarke, L.A., and Hayden, M.R. (1993). A PCR method for accurate assessment of trinucleotide repeat expansion in Huntington disease. Hum. Mol. Genet. *2*, 635–636.

Huntington's Disease Collaborative Research Group (1993). A novel gene containing a trinucleotide repeat that is expanded and unstable on Huntington's disease chromosomes. Cell *72*, 971–983.

Ide, K., Nukina, H., Masuda, N., Goto, J., and Kanazawa, I. (1995). Abnormal gene product identified in Huntington's disease lymphocytes and brain. Biochem. Biophys. Res. Commun. *209*, 1119–1125.

Koenig, H. (1974). The isolation of lysosomes from brain. In Methods in Enzymology, Vol. 31, Biomembranes (Part A), S. Fleisher and L. Packer, eds. (New York: Academic Press), pp. 457–477.

MacDonald, M.E., Barnes, G., Srinidhi, J., Duyao, M.P., Ambrose, C.M., Myers, R.H., Gray, J., Conneally, P.M., Young, A., Penney, J., et al. (1993). Gametic but not somatic instability of CAG repeat length in Huntington's disease. J. Med. Genet. *30*, 982–986.

Morishima-Kawashimia, M., Hasegawa, M., Takio, K., Suzuki, M., Titani, K., and Ihara, Y. (1993). Ubiquitin is conjugated with amino-terminally processed tau in paired helical filaments. Neuron *10*, 1151–1160.

Nasir, J., Floresco, S.B., O'Kusky, J.R., Diewert, V.M., Richman, J.M., Zeisler, J., Borowski, A., Marth, J.D., Phillips, A.G., and Hayden, M.R. (1995). Targeted disruption of the Huntington's disease gene results in embryonic lethality and behavioral and morphological changes in heterozygotes. Cell *81*, 811–823.

Perutz, M.F., Johnson, T., Suzuki, M., and Finch, J.T. (1994). Glutamine repeats as polar zippers: their possible role in inherited neurodegenerative diseases. Proc. Natl. Acad. Sci. USA *91*, 5355–5358.

Servadio, A., Koshy, B., Armstrong, D., Antalffy, B., Orr, H.T., and Zoghbi, H.Y. (1995). Expression analysis of the ataxin-1 protein in tissues from normal and spinocerebellar ataxia type 1 individuals. Nature Genet. *10*, 94–98.

Sharp, A.H., Loev, S.J., Schilling, G., Li, S.-H., Li, X.-J., Bao, J., Wagster, M.V., Kotzuk, J.A., Steiner, J.P., Lo, A., et al. (1995). Widespread expression of Huntington's disease gene (IT15) protein product. Neuron *14*, 1065–1074.

Snell, R.G., MacMillan, J.C., Cheadle, J.P., Fenton, I., Lazarou, L.P., Davies, P., MacDonald, M., Gusella, J.F., Harper, P.S., and Shaw, D.J. (1993). Relationship between trinucleotide repeat expansions and phenotypic variation in Huntington's disease. Nature Genet. *4*, 393–397.

Stine, O.C., Pleasant, N., Franz, M.L., Abbott, M.H., Folstein, S.E., and Ross, C.A. (1993). Correlations between the onset age of Huntington's disease and length of the trinucleotide repeat in IT15. Hum. Mol. Genet. *2*, 1547–1549.

Stine, O.C., Li, S.-H., Pleasant, N., Wagster, M.V., Hedreen, J.C., and Ross, C.A. (1995). Expression of the mutant allele of IT-15 (the HD gene) in striatum and cortex of Huntington's disease patients. Hum. Mol. Genet. *4*, 15–18.

Telenius, H., Kremer, B., Goldberg, Y.P., Theilmann, J., Andrew, S.E.,

Zeisler, J., Adam, S., Greenberg, C., Ives, E.J., Clarke, L.A., and Hayden, M.R. (1994). Somatic and gonadal mosaicism of the Huntington disease gene CAG repeat in brain and sperm. Nature Genet. *6*, 409–414.

Trottier, Y., Devys, D., Imbert, G., Saudou, F., An, I., Luta, Y., Weber, C., Agid, Y., Hirsch E.C., and Mandel, J.-L. (1995). Cellular localization of the Huntington's disease protein and discrimination of the normal and mutated form. Nature Genet. *10*, 104–110.

Ueno, S., Kondoh, K., Kotani, Y., Komure, O., Kuno, S., Kawai, J., Hazama, F., and Sano, A. (1995). Somatic mosaicism of CAG repeat in dentatorubral-pallidoluysian atrophy (DRPLA). Hum. Mol. Genet. *4*, 663–666.

Vonsattel, J.-P., Myers, R.H., Stevens, T.J., Ferrante, R.J., Bird, E.D., and Richardson, E.P., Jr. (1985). Neuropathological classification of Huntington's disease. J. Neuropathol. Exp. Neurol. *44*, 559–577.

Wexler, N.S., Young, A.B., Tanzi, R.E., Travers, H., Starosta-Rubenstein, S., Penney, J.B., Snodgrass, S.R., Shoulson, I., Gomez, F., Ramos Arroyo, M.S., et al. (1987). Homozygotes for Huntington disease. Nature *326*, 194–197.

Willems, P.J. (1994). Dynamic mutations hit double figures. Nature Genet. *8*, 213–215.

Yazawa, I., Nukina, N., Hashida, H., Goto, J., Yamada, M., and Kanazawa, I. (1995). Abnormal gene product identified in hereditary dentatorubral-pallidoluysian atrophy (DRPLA) brain. Nature Genet. *10*, 99–103.

Young, A.B. (1994). Huntington's disease: lessons from and for molecular neuroscience. Neuroscientist November, 30–37.

Zuhlke, C., Riess, O., Bockel, B., Lange, H., and Thies, U. (1993). Mitotic stability and meiotic variability of the $(CAG)_n$ repeat in the Huntington disease gene. Hum. Mol. Genet. *2*, 2063–2067.